

Infrared survey of the carrier dynamics in III-V digital ferromagnetic heterostructuresK. S. Burch,^{1,*} E. J. Singley,^{1,†} J. Stephens,² R. K. Kawakami,^{2,‡} D. D. Awschalom,² and D. N. Basov¹¹*Department of Physics, University of California, San Diego, California 92093-0319, USA*²*Center for Spintronics and Quantum Computation, University of California, Santa Barbara, California 93106, USA*

(Received 28 April 2004; revised manuscript received 30 November 2004; published 31 March 2005)

We report on the electromagnetic response of digital ferromagnetic heterostructures (DFH): systems with δ -doped MnAs layers separated by GaAs spacers of variable thickness (y). The gross features of the infrared conductivity of DFH samples are consistent with the notion that these digital structures are GaAs/Ga_{1-x}Mn_xAs superlattices. This conclusion is supported by a combination of spectral weight analysis and effective medium theory. The optical properties of DFH also provide insights into the evolution of their critical temperature with GaAs spacing. In DFH a low-lying gap materializes in the energy dependent conductivity, which is interpreted as a mobility gap resulting from Anderson localization.

DOI: 10.1103/PhysRevB.71.125340

PACS number(s): 78.67.Pt, 72.20.Ee, 75.50.Pp, 78.30.Fs

I. INTRODUCTION

For decades semiconductor superlattices have offered experimental access to structures with tailored transport properties thus providing one with a unique laboratory to explore the rich electronic behavior of these systems.¹ Recently this approach was employed to create a new class of III-V, Mn doped, dilute magnetic semiconductors (DMS) that promise to advance our understanding of the interplay between dimensionality, carrier dynamics, and magnetism in this family of materials.^{2,3} These phenomena are difficult to investigate using random alloys due to the multiple effects of Mn doping. Apart from generating local moments and carriers (holes), Mn introduces disorder with all these effects revealing non-trivial entanglement.⁴

In digital ferromagnetic heterostructures (DFH) these problems may be overcome by holding the Mn density constant while varying the spacing between δ -doped layers. Indeed, DFHs are comprised of δ -doped MnAs submonolayers separated by GaAs spacers of variable thickness (y).^{2,3} To take full advantage of the DFH approach it is prudent to inquire into the nature of the doped layers as well as the electronic and/or magnetic coupling between them. Empowered by earlier spectroscopic studies of the Ga_{1-x}Mn_xAs random alloys⁵ we demonstrate that the doped layer in DFHs possesses the properties of Ga_{1-x}Mn_xAs. Furthermore, these digital structures enable access to the doping regime previously unattainable in the random alloy. We have combined effective medium theory with the sum rules to quantitatively evaluate the evolution of the electronic response with y . This analysis clearly demonstrates that the development of the transport properties of DFH are due to intrinsic changes in the doped layer and not the result of compensation from the spacer layer. The optical properties of DFH also offer insights into the origin of the suppression of the critical temperature and development of the insulating state with increased spacer thickness.^{2,3} We find that the latter effect occurs due to the diminished coupling between Ga_{1-x}Mn_xAs layers without apparent depression of the electronic spectral weight associated with the doped holes within the layers. Charge carriers become increasingly localized at $y \geq 15$

monolayers (ML) prompting a mobility gap, which has never previously been observed to coexist with ferromagnetism in III-V semiconductors.

II. EXPERIMENTAL PROCEDURES AND RAW DATA

The DFH used in this study were grown at UCSB on semi-insulating GaAs (100) by low temperature molecular beam epitaxy (LT-MBE). This series of DFH included samples with one half monolayer (1 ML \cong 2.84 Å) MnAs separated by LT-GaAs spacers of various thickness. Previous studies have demonstrated that the Mn diffuses 3–5 ML into the GaAs matrix.² The samples were characterized using a SQUID magnetometer, showing a well defined hysteresis loop below the ferromagnetic transition temperature (T_C). These DFH followed the general trend of a reduction in T_C with increasing y until ≈ 50 ML where T_C becomes independent of y (see Table I).² Near normal incidence, $\vec{E} \perp \hat{z}$ (growth direction), transmission $T(\omega)$ and reflection $R(\omega)$ measurements were carried out at UCSD in the range 15–12000 cm⁻¹ (≈ 1 meV to ≈ 1.5 eV, the band gap of GaAs). $T(\omega)$ was measured between 5 and 292 K. The real and imaginary parts of the complex conductivity $\hat{\sigma}(\omega) = \sigma_1 - i\sigma_2$, were determined through Kramers-Kronig analysis and confirmed at room temperature by direct derivation from $T(\omega)$ and $R(\omega)$.^{5,6}

TABLE I. Parameters of the DFH studied. All samples were grown at a substrate temperature of 265 C, with As/Mn beam flux ratio of $\sim 200/1$. Ga growth rates were ~ 0.3 ML/s and Mn growth rates were 0.02–0.05 ML/s. Further details can be found in Ref. 2.

y (ML)	Total layers	T_C (K)
10	153	55
15	100	48.5
20	100	38
25	63	36
25	200	36
70	23	30

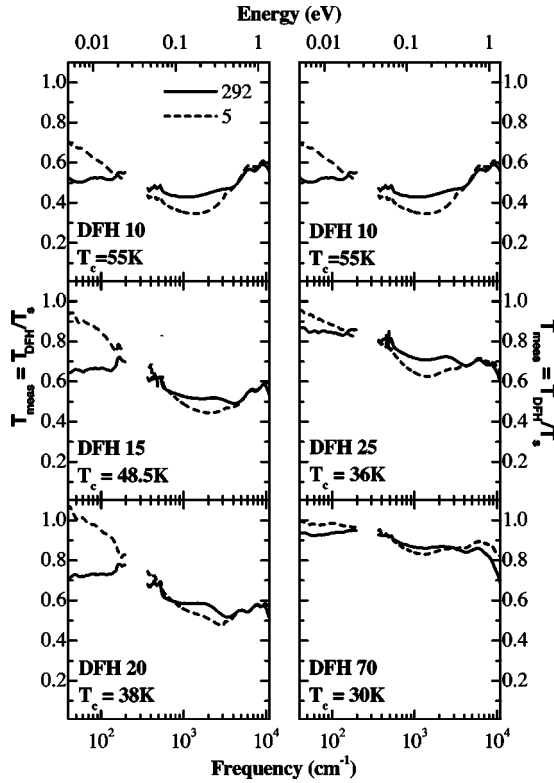


FIG. 1. The raw transmission data for five of the samples in this study. Displayed is the transmission through the DFH samples that has been divided by the transmission through a GaAs substrate ($T_{meas} = T_{DFH}/T_s$) at 292 K and 5 K. Deviations of T_{meas} from 1 is an indication of absorption in the DFH film. The left panel compares three DFH samples with increasing spacer thickness. While the dip in the midinfrared ($\approx 2000 \text{ cm}^{-1}$) grows at low temperatures, the far infrared absorption is dramatically reduced at 5 K. This effect is more accurately portrayed in the right panel for the three films with similar thickness. The weak oscillations observed throughout the frequency range in all samples are due to interference within the film.

In Fig. 1 we plot the transmission spectra of DFH superlattices normalized by transmission through the GaAs substrate ($T_{meas} = T_{DFH}/T_s$) for representative samples.⁷ In the left panel we explore the general trends with changes to the GaAs spacer thickness. All three samples show a dip centered at $\omega \approx 2000 \text{ cm}^{-1}$, of approximately the same strength. These samples also show a substantial drop in T_{meas} above $\omega \approx 7000 \text{ cm}^{-1}$ which is an indication of a broadening of the GaAs band edge. In the far infrared (low energy portion of the spectra) absorption is clearly reduced with increased spacer thickness. In order to make a quantitative comparison between the raw transmission spectra, it is instructive to compare samples of similar thickness. In the right panel of Fig. 1 we plot the transmission spectra for DFH 10, 25, and 70 ML spacer with the total number of doped layers chosen such that they all have the same total thickness of the superlattice sample ($\approx 460 \text{ nm}$). In this panel we see the dramatic effect of increasing spacer thickness: a significant increase in transmission throughout the frequency range measured. Turning to the temperature dependence of these heterostructures, the far infrared absorption is reduced at low tempera-

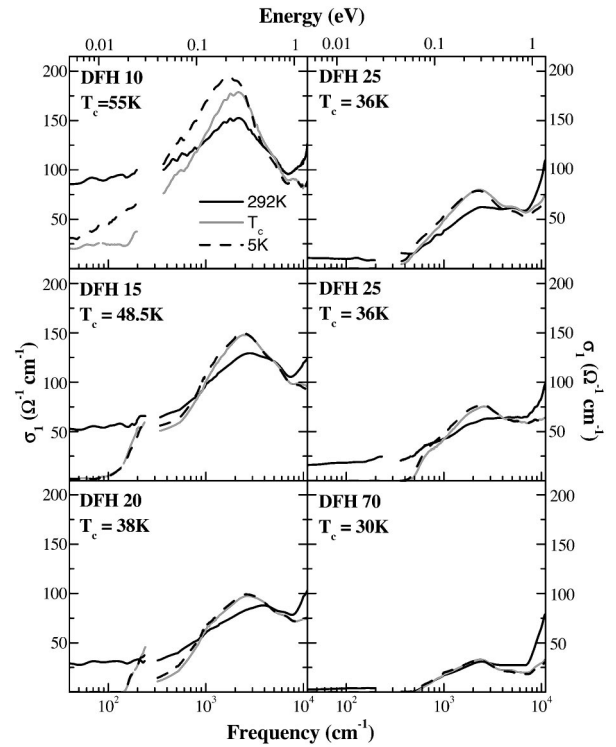


FIG. 2. The real part of the frequency dependent conductivity [$\sigma_1(\omega)$] for all digital ferromagnetic heterostructures studied. Shown here are spectra at room temperature (292 K), the ferromagnetic transition temperature (T_C), and the lowest temperature studied (5 K). All samples reveal a resonance at $\omega \approx 2000 \text{ cm}^{-1}$ and band tailing at high frequencies due to defects. The free carrier component is reduced with increasing spacer thickness and decreasing temperature, until T_C . For all digital samples with a GaAs spacer thickness greater than 10 ML, a new feature emerges: a low lying gap in $\sigma_1(\omega)$ developing at low temperature.

tures while the $\omega \approx 2000 \text{ cm}^{-1}$ dip is enlarged. The effect of temperature in the far infrared $T(\omega)$ is especially dramatic in samples with GaAs spacers $\geq 15 \text{ ML}$. The dip in the mid infrared transmission data produces a clear resonance feature in the Kramers-Kronig generated $\sigma_1(\omega)$ discussed below.

III. CONDUCTIVITY DATA AND SPECTRAL WEIGHT ANALYSIS

In Fig. 2, the dissipative part of the optical conductivity [$\sigma_1(\omega)$] is plotted for all DFH samples in this study. In all digital structures we see a resonance at $\omega \approx 2000 \text{ cm}^{-1}$ that has a similar shape as the interband absorption feature observed in ferromagnetic $\text{Ga}_{1-x}\text{Mn}_x\text{As}$ alloys.^{5,8} At higher energies all samples display a similar smearing of the band edge, characteristic of GaAs grown by LT-MBE.⁵ As y is increased the overall magnitude of the conductivity is reduced. Examining the far infrared region, where spectral weight is primarily due to mobile carriers, one observes that the relative strength of $\sigma_1(\omega \rightarrow 0)$ in relation to the mid infrared resonance is reduced as y is increased. In the low temperature spectra, the far infrared conductivity is de-

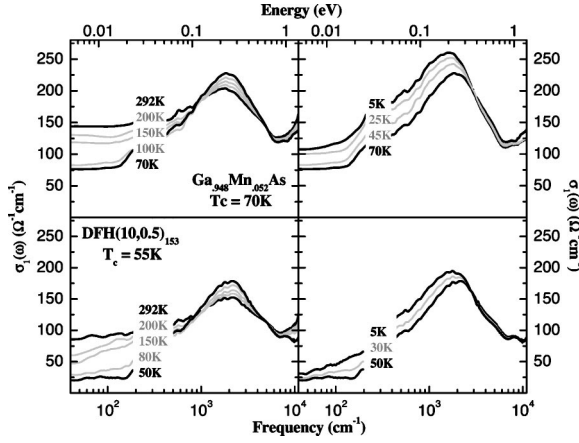


FIG. 3. Temperature dependence of $\sigma_1(\omega)$ for DFH with $y=10$ ML (bottom panels) and $\text{Ga}_{0.948}\text{Mn}_{0.052}\text{As}$ random alloy (top panels). On the left we show data at temperatures from 292 K to T_C , and on the right $\sigma_1(\omega)$ spectra from T_C to 5 K. A resonance near 2000 cm^{-1} which grows as the temperature is lowered can be seen in all of the spectra. Additionally as the temperature is lowered until T_C the free carrier part is reduced, and then grows slightly below T_C .

pressed below our detection limit ($\approx 1 \text{ } \Omega^{-1}\text{cm}^{-1}$) in all DFH samples with $y \geq 15$ ML, suggesting the opening of a low lying energy gap. The magnitude of this gap in $\sigma_1(\omega)$ appears to increase from $\approx 200 \text{ cm}^{-1}$ to 500 cm^{-1} as y is varied from 15 to 70 ML.⁹ The gap develops as the temperature is reduced, and indicates no anomalies at T_C . This low energy gap signifies an important change in the dynamic properties of the states at and around the Fermi level (E_F), as discussed in Sec. IV B

To investigate the result of digital doping, we compare in Fig. 3 the data for the 10 ML sample with that of an alloy having the same bulk Mn concentration ($\text{Ga}_{0.948}\text{Mn}_{0.052}\text{As}$). The temperature dependence of the conductivity reveals similar trends for both the alloy and the DFH. In the paramagnetic state ($T > T_C$, left panels) the strength of $\sigma_1(\omega \rightarrow 0)$ is weakened as T is lowered in both materials. However, for $T < T_C$ (right panels), both the 10 ML DFH and $\text{Ga}_{0.948}\text{Mn}_{0.052}\text{As}$ samples recover some of their low energy spectral weight. The common characteristics in the energy and temperature dependence of $\sigma_1(\omega)$ in DFHs and the random alloys strongly suggest that digital doping of MnAs in GaAs produces heavily doped layers of $\text{Ga}_{1-x}\text{Mn}_x\text{As}$ spaced by GaAs. This is consistent with recent x-ray and TEM studies of similar samples that demonstrate Mn are doped in a Ga site and spread out between 3 and 5 ML.^{2,11} As will be shown below, this conclusion is also supported by the spectral weight analysis.

The evolution of the electronic response of DFHs with the increase of the GaAs spacer thickness is well described by the effective medium theory (EMT). EMT allows one to predict the electromagnetic response of a superlattice from the optical constants of its constituents.¹⁰ Given the geometry of our measurements ($\vec{E} \perp$ to the growth axis), the experimental conductivity can be written as

$$\sigma_1(\omega) = \left(\frac{d_{el}}{d_{total}} \right) \sigma_1^{el}(\omega) + \left(\frac{d_{GaAs}}{d_{total}} \right) \sigma_1^{GaAs}(\omega), \quad (1)$$

where d_a is the thickness of layer a , d_{total} is one period of the superlattice, and “el” refers to the effective layer produced by the Mn doping.¹² For this study it was assumed that $\sigma_1^{GaAs}(\omega)$ is the same as previously measured for GaAs grown by LT-MBE (LT-GaAs).⁵ One key feature of LT-GaAs is $\sigma_1^{GaAs}(\omega \leq 7000 \text{ cm}^{-1}) \approx 0$, [see Eq. (1) and Fig. 6] implying that the conductivity of the superlattice can be written as $\sigma_1(\omega \leq 7000 \text{ cm}^{-1}) = (d_{el}/d_{total})\sigma_1^{el}(\omega)$. Therefore throughout most of the intragap region EMT has the net effect of rescaling the $\sigma_1(\omega)$ spectra. In order to verify that the gross features of the data are consistent with the EMT prediction, we focus on the integrated spectral weight, $N_{eff} = \int_0^{\Omega_c} \sigma_1(\omega) d\omega$,¹³ which is proportional to the density of carriers responsible for the strength of $\sigma_1(0 < \omega < \Omega_c)$. For clarity we have adopted the notation N_{eff}^{meas} for the measured spectral weight and N_{eff}^{el} for the intrinsic spectral weight of a doped layer. In the spirit of the EMT it is instructive to examine the ratio of the integrals for samples with GaAs spacer thickness A and B yielding

$$\frac{[N_{eff}^{meas}]_A}{[N_{eff}^{meas}]_B} = \frac{\int_0^{\Omega_c} [\sigma_1(\omega)]_A d\omega}{\int_0^{\Omega_c} [\sigma_1(\omega)]_B d\omega} = \frac{[d_{total}]_B}{[d_{total}]_A} \times \frac{[d_{el}N_{eff}^{el}]_A}{[d_{el}N_{eff}^{el}]_B}. \quad (2)$$

The result of this analysis at $T=5 \text{ K}$ with the $y=10$ ML sample used as a reference are plotted in Fig. 4.¹⁴ To compare these results with the EMT prediction, we also plot the ratio of the periods of each sample ($y/10$). The excellent agreement between the EMT prediction for the rescaling of spectral weight due to increased insulator thickness y , and $[N_{eff}^{meas}(5 \text{ K})]_{10}/[N_{eff}^{meas}(5 \text{ K})]_y$ can be clearly seen in Fig. 4.

IV. DISCUSSION

A. Spectroscopic signatures of DFH as a superlattice of $\text{Ga}_{1-x}\text{Mn}_x\text{As}/\text{GaAs}$

Data presented in Sec. III strongly suggest that digital doping results in a heavily doped layer of $\text{Ga}_{1-x}\text{Mn}_x\text{As}$ separated by undoped spacers of LT-GaAs. Specifically the shape and position of the midinfrared resonance is consistent with the interband transitions observed in $\text{Ga}_{1-x}\text{Mn}_x\text{As}$ alloys.^{5,8} Additionally the broadening of the band edge extends to lower frequencies and has greater strength than what is found in LT-GaAs, yet is similar to what is found in $\text{Ga}_{1-x}\text{Mn}_x\text{As}$ alloys. In fact this is a key spectroscopic signature of defects in $\text{Ga}_{1-x}\text{Mn}_x\text{As}$ ⁵ and therefore the band-broadening seen in DFH suggests the doped layers have a band structure similar to that found in $\text{Ga}_{1-x}\text{Mn}_x\text{As}$ alloys. Furthermore the temperature dependence of the far or midinfrared features is consistent with the conclusion that the electronic behavior of DFH samples is that of $\text{Ga}_{1-x}\text{Mn}_x\text{As}/\text{LT-GaAs}$ superlattice.

However, another possibility exists, namely that the doped layers of DFH are primarily MnAs clusters. If the DFH contained MnAs precipitates in GaAs, the effective me-

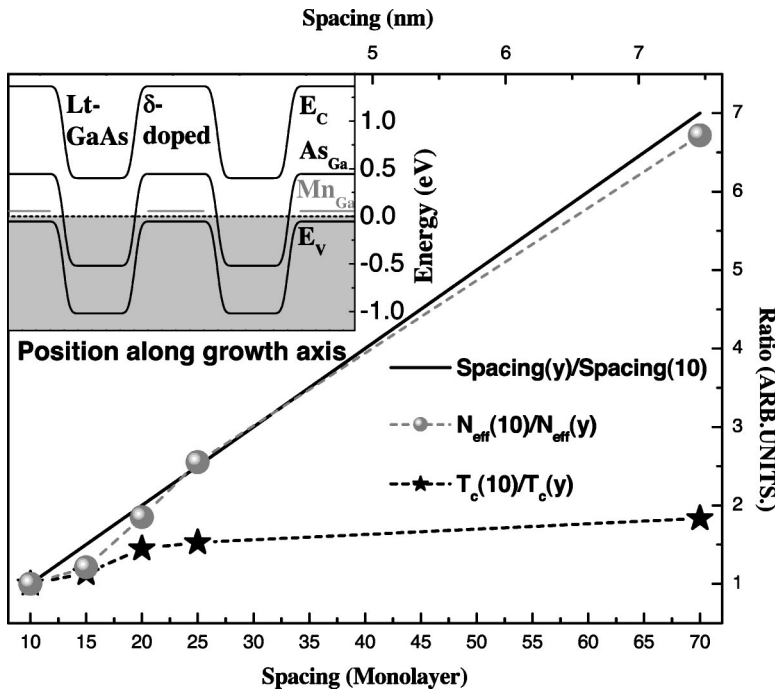


FIG. 4. N_{eff}^{meas} ratios, as defined in the text, of all DFHs studied versus the EMT prediction [see Eq. (2)] along with the T_C ratios (Ref. 13). In the inset we show a schematic representation of the band critical points versus position along the growth axis. $E_{C,V}$ are the conduction (valence) band minima (maxima). Also displayed are the positions of the intragap levels produced by both Mn and As substitution on a Ga site.

dium approximation can be employed to predict the measured $\sigma_1(\omega)$ from the optical properties of MnAs and GaAs. To apply this theory we have performed reflectance and ellipsometric spectroscopy on epitaxially grown MnAs on GaAs. We have extracted the optical conductivity of MnAs by fitting the data for a MnAs/GaAs structure with the Drude model augmented with a set of Lorentzian oscillators. Details of this analysis shall be given in a later publication, however the results are quantitatively consistent with previous optical studies of single crystal MnAs and $\sigma_1(\omega \rightarrow 0)$ agrees well with the dc resistivity of epitaxial MnAs.^{16,17} Using this fit, and our previous results for LT-GaAs (see Ref. 5) we have utilized the Bruggeman theory (better known as the effective medium approximation) to predict the optical

properties of MnAs precipitates.¹⁸ The measured conductivity of MnAs as well as the results of the effective medium approximation are plotted in Fig. 5. Assuming a filling fraction of the MnAs of 0.16 to 0.10, corresponding to 3–5 ML spread, we find no free carrier absorption and a resonance centered at $10\,000\text{ cm}^{-1}$. Additionally the strength of the resonance is an order of magnitude stronger than the $\sigma_1^{el}(\omega)$ of the DFH (the details of the determination of $\sigma_1^{el}(\omega)$ are given at the end of this section). Therefore we believe MnAs precipitates play little or no role in the optical response of DFH. This further supports the conclusion that in the doped layer of DFH samples the Mn has incorporated itself in the GaAs matrix in a similar fashion as in the random alloy. We also note that these results are consistent with magnetization

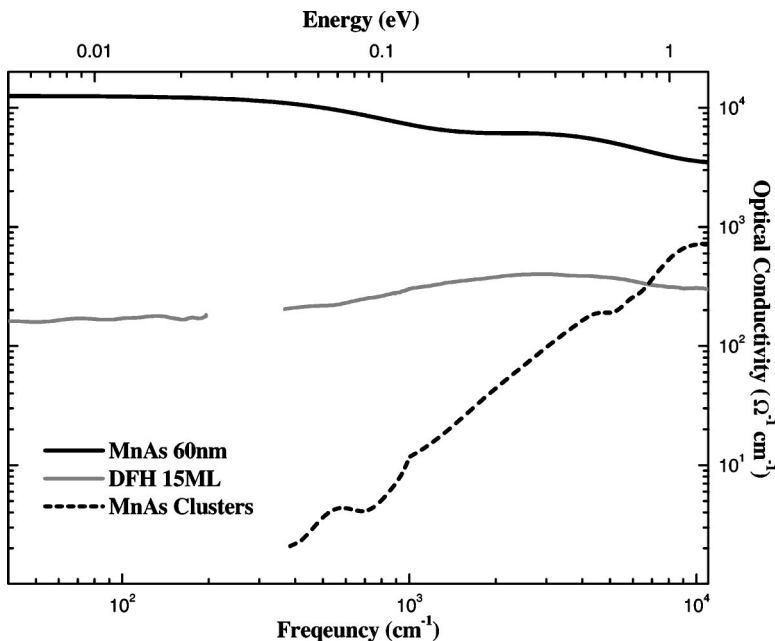


FIG. 5. The experimental conductivity at 292 K of a MnAs thin film is compared with the intrinsic conductivity of $\sigma_1^{el}(\omega)$ of the DFH with 15 ML spacing. Conductivity due to MnAs clusters in LT-GaAs has been simulated using the effective medium approximation (Refs. 12 and 18). In extracting the conductivity for DFH 15 ML and generating the response of the MnAs clusters, it was assumed that the MnAs diffused 5 ML. Noting the log-log scale, there is a significant difference between the results for the clusters model and the extracted conductivity for a single doped layer in DFH.

data that shows no remnant magnetization at 300 K, whereas MnAs is well known to have a $T_C \approx 310$ K.

Another possibility worthy of exploration, is the result of Mn completely diffusing into the LT-GaAs. To explore this possibility we return to Fig. 4, where the agreement between the EMT prediction ($N_{eff}^{meas} \propto 1/y$) and the spectral weight results is shown. It is interesting to note that the prediction of the EMT for a $\text{Ga}_{1-x}\text{Mn}_x\text{As}/\text{LT-GaAs}$ is exactly what one might expect from a $\text{Ga}_{1-x}\text{Mn}_x\text{As}$ random alloy. Namely as the undoped portion of the superlattice is increased, the average density of the carriers (acceptors) throughout the material is reduced. However, LT-GaAs is n -type, due to the presence of arsenic antisites (As_{Ga}) double donors. Therefore if the Mn completely diffused throughout the sample, as y is increased these antisites would lead to additional compensation in the material. This would ultimately result in $N_{eff}^{meas} \propto 1/y^\alpha$, with $\alpha \gg 1$. As we discuss below, the conservation of spectral weight with increased LT-GaAs spacer is only possible in a superlattice due to the confinement electrons or holes produced by this “artificial” structure. Therefore based on the comparison with the random alloy, the spectral weight analysis, MnAs EMA analysis and EMT results, we conclude that DFHs have the electronic signatures of a superlattice of $\text{Ga}_{1-x}\text{Mn}_x\text{As}/\text{GaAs}$.

Several implications of the above findings are worthy of attention. First, based on the superlattice conclusion, one can infer the energy bands diagram for a $\text{Ga}_{1-x}\text{Mn}_x\text{As}/\text{GaAs}$ structure as a function of position along the growth axis (see inset of Fig. 4). Since LT-GaAs contains electrons and $\text{Ga}_{1-x}\text{Mn}_x\text{As}$ has holes, the DFHs form a periodic array of pn -junctions. The miss-match in the positions of E_F in the neighboring layers by at least 0.5 eV results in significant band bending. Hence Mn induced holes and As_{Ga} induced electrons will experience an electrostatic potential along the growth direction confining them in their corresponding layers. This confinement accounts for the diminished capacity of As_{Ga} to compensate holes in DFH systems. Indeed the EMT analysis demonstrates that N_{eff}^{meas} scales with y for $\omega \leq 4500 \text{ cm}^{-1}$. This result implies that N_{eff}^{el} , and therefore the number of holes within the doped layers, is not significantly affected by increased spacer thickness. Therefore changes in $\sigma_1(\omega)$ as y is increased cannot be due to compensation. Since the spectral weight in the far infrared region results from intraband transitions, the opening of a low energy gap must be the result of significant change in the nature of the states at the Fermi energy. Furthermore, since N_{eff}^{el} is constant with y , the loss of spectral weight at low energies must result in an increase in spectral weight in the mid infrared [as $N_{eff}^{el} = \int_0^{4000 \text{ cm}^{-1}} \sigma_1^{el}(\omega) d\omega$]. Indeed, in our previous study of the random alloy we determined that as the doping level was reduced the strength of both the far and midinfrared absorption was depleted.⁵ Therefore the simultaneous existence of a low energy gap and mid infrared resonance is clearly a result of the digital superlattice.

We further explore the trends in DFHs spectra, using the EMT analysis to extract the response of a single doped layer [$\sigma_1^{el}(\omega)$, see Fig. 6]. To generate this data set we have assumed $d_{el} = 5$ ML, noting that this is most likely an overestimate, although it results in a conservative measure of

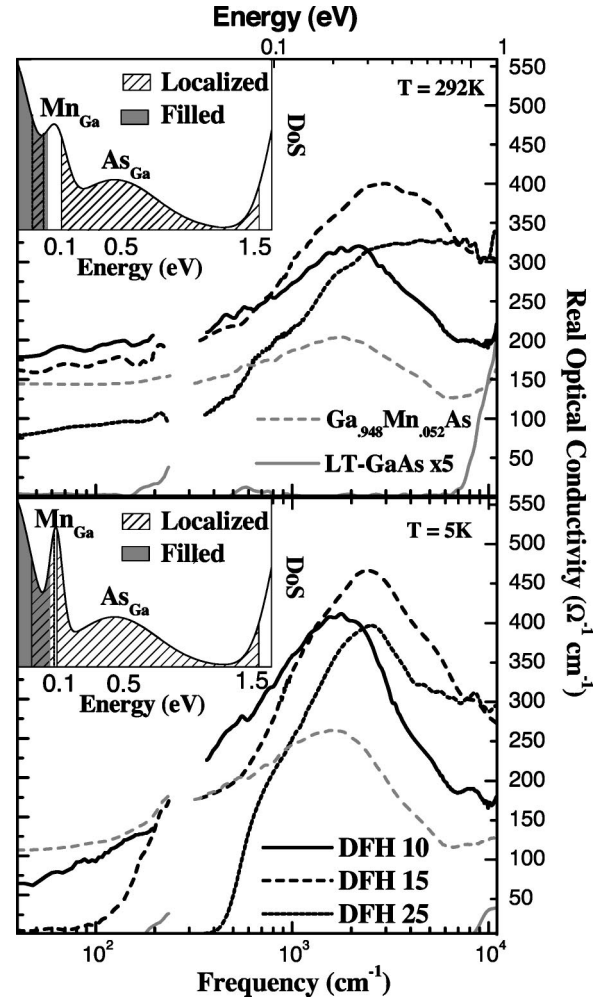


FIG. 6. The effective conductivity of a doped layer [$\sigma_1^{el}(\omega)$] extracted using the EMT analysis of raw data as described in the text. The top panel shows the result at 292 K and in the bottom panel 5 K results are plotted. Also shown are $\sigma_1(\omega)$ for $\text{Ga}_{0.948}\text{Mn}_{0.052}\text{As}$ and $\sigma_1(\omega) \times 5$ for LT-GaAs.

$\sigma_1^{el}(\omega)$.¹⁵ Apart from the far infrared region, the overall strength of the optical conductivity has been equalized as the result of the EMT analysis. It is instructive to compare $\sigma_1^{el}(\omega)$ for digital structures with $\sigma_1(\omega)$ of $\text{Ga}_{0.948}\text{Mn}_{0.052}\text{As}$. It is apparent from Fig. 6 that the overall oscillator strength of the mid-infrared resonance in all DFHs is significantly larger than in $\text{Ga}_{0.948}\text{Mn}_{0.052}\text{As}$. Furthermore the spectral weight for the DFH systems exceeds the N_{eff} values for the alloys with similar bulk content of Mn by a factor of 2–3 (depending on the choice of d_{el}). Using previously determined values for the effective mass in $\text{Ga}_{1-x}\text{Mn}_x\text{As}$ ⁵ and assuming $d_{el} = 5$ ML, we find the carrier density is between $2.9 \times 10^{20} \text{ cm}^{-3}$ and $1.4 \times 10^{21} \text{ cm}^{-3}$. This result shows that the DFH approach enables one to achieve doping levels not readily attainable in three dimensional alloys.

B. Ferromagnetism in DFHs

The suppression of T_C in DFHs compared to that of alloys near optimal Mn doping, is surprising. In previous studies of

$\text{Ga}_{1-x}\text{Mn}_x\text{As}$ it was established that T_C correlates with the doping-induced spectral weight.⁵ Additionally other recent experimental results for $\text{Ga}_{1-x}\text{Mn}_x\text{As}$ have held that a larger carrier concentration produces a higher T_C .^{4,19-21} To further explore this relation in DFHs, we have plotted the ratio of $T_c(10)/T_c(y)$ in Fig. 4. We expect $T_c(10)/T_c(y)=1$, since the $N_{\text{eff}}^{\text{el}}$ intrinsic to the doped layer is constant. Contrary to this conjecture, T_C is reduced with increased y . Insights into the evolution of T_C with y are provided by examining σ_1^{el} in the limit of $\omega \rightarrow 0$, noting that the response in this region is dominated by intra-band transitions. Here we find a depression of the conductivity in DFH with $y=10$ ML compared to that of $\text{Ga}_{0.948}\text{Mn}_{0.052}\text{As}$ (see Fig. 2). As y is increased, a low-lying gap develops and T_C continues to drop. We therefore conclude that the carrier dynamics, and not simply the hole density, plays an important role in defining the ferromagnetic properties of $\text{Ga}_{1-x}\text{Mn}_x\text{As}$.

To gain a better understanding of the role of hole dynamics on the ferromagnetic state in DFH, it is important to elucidate the physical mechanism leading to the low-lying energy gap in $\sigma_1^{\text{el}}(\omega)$. The data presented here are consistent with the conclusion that the gap is produced by E_F entering a region of localized states within a mobility gap.²² The insets of Fig. 6, schematically show the density of states of Mn-doped GaAs. The top inset corresponds to the metallic random alloys and may be applicable to the DFH sample with $y=10$ ML. Depicted in the inset is a fairly broad Mn induced impurity band hybridized with the GaAs valence band, consistent with a number of recent experiments^{5,19,23} and band structure calculations.²⁴ The bottom inset displays the consequence of increasing the GaAs spacer thickness, which results in a reduction of the overlap of the hole wave functions and therefore diminishes the width of the impurity band (D). A repercussion of a smaller D is an increase in the fraction of localized states, placing E_F in a mobility gap.^{22,25} Since the holes are strongly localized in DFH with $y \geq 15$ ML they can support current primarily through variable range hopping leading to a dramatic reduction of $\sigma_1(\omega \rightarrow 0)$. At finite temperatures the low-energy spectral weight is expected to be enhanced due to activation across the mobility gap in accord with both our data (see Figs. 2 and 6) and dc results (see Ref. 3). To the best of our knowledge this work is the first experimental study where the opening of a sizable mobility gap is prompted by dimensionality alone without altering either the carrier density or disorder within the conducting layers. The changes in the Mn impurity band that result in the opening of a mobility gap are also likely to be responsible for the concurrent changes in T_C . Namely, as the doped layers become isolated from one another, the impurity band width is reduced and there is a reduction in the kinetic energy of the holes. Therefore less energy is available to compensate the loss of entropy as the sample enters the ferromagnetic state. This will inevitably result in a reduction of the temperature at which there is a minimum in the free energy, and hence T_C is lowered.^{26-28,30}

V. SUMMARY AND OUTLOOK

In this study we have examined the optical properties of digital ferromagnetic heterostructures. From our detailed

analysis of the the optical conductivity of DFHs and $\text{Ga}_{1-x}\text{Mn}_x\text{As}$ three dimensional alloys, the evolution of the spectral weight with y , and the possibilities of metallic clusters, we have concluded DFHs are superlattices of $\text{Ga}_{1-x}\text{Mn}_x\text{As}/\text{GaAs}$. The results presented here are incongruent with a picture of a doped layer of MnAs clusters. Namely the resonance at 2000 cm^{-1} matches the interband absorption seen in the random alloys, and is too low in energy to be due to MnAs precipitates. As the GaAs spacer thickness is increased, the infrared data uncover a low-lying mobility gap in the electromagnetic response of DFH systems. The magnitude of the gap systematically increases with spacer thickness, while T_C and the measured $\sigma_1(\omega)$ are suppressed. Evolution of $\sigma_1(\omega)$ data with increasing GaAs spacer thickness is in accord with the effective medium theory. Thus it appears that the origin of the changes in the transport properties of DFHs are due to a reduction in the impurity bandwidth, which in turn results in enhanced localization of the holes.

Our findings reinforce the notion of a ferromagnetic state mediated by Anderson localized holes in the Mn induced impurity band. Tunability of the impurity bandwidth without apparent change of doping level offers previously unexplored controls of the magnetic state in III-V ferromagnetic superlattices. Specifically DFHs allow us to test the predictions of the importance of the impurity band width in the ferromagnetism of $\text{Ga}_{1-x}\text{Mn}_x\text{As}$.²⁶⁻²⁹ The electrostatic confinement in the growth-direction inferred from the electronic structure of DFHs implies that carrier mediated magnetic coupling between the doped layers is unlikely, providing a challenge to current models of ferromagnetism in DFHs.³⁰ Nonetheless our findings clearly support the underlying assumption of ferromagnetism mediated by strongly confined holes, and therefore suggests that these theoretical studies may have captured the basic physics for a single digitally doped layer.

Further studies are clearly required to quantitatively understand the changes in T_C with y . Specifically an experimental determination of the localization length and impurity band width in different DFHs will guide the development of an accurate theoretical description of these materials. Nonetheless this work is the first demonstration of ferromagnetism in heavily doped $\text{Ga}_{1-x}\text{Mn}_x\text{As}$ coexisting with a prominent mobility gap, a hallmark of an Anderson insulator. Finally we remark on the exciting prospect offered by the data in Figs. 1 and 2. Despite the significant differences in absorption, DFHs with 10 and 15 ML spacings have similar magnetic properties. This not only demonstrates the complicated nature of the ferromagnetic state in $\text{Ga}_{1-x}\text{Mn}_x\text{As}$ but offers a unique opportunity to tune the optical, transport and magnetic properties of dilute magnetic semiconductors using novel growth techniques, such as digital doping.

ACKNOWLEDGMENTS

This work was supported by the DOE, NSF, DARPA, and ONR. We are grateful for numerous discussions with C.Ciuti, L. Cywinski, M. Fogler, B.H. Lee, A. MacDonald, J. McGuire, S. Das Sarma, L.J. Sham, and J. Sinova.

- *Electronic address: burch@physics.ucsd.edu
 †Permanent address: Department of Physics, California State University, Hayward, CA 94542.
 ‡Permanent address: Department of Physics, University of California, Riverside, CA 92521.
- ¹P. Y. Yu and M. Cardona, *Fundamentals of Semiconductors* (Springer-Verlag, Berlin, 1996).
 - ²R. K. Kawakami, E. Johnston-Halperin, L. F. Chen, M. Hanson, N. Gubels, J. S. Speck, A. C. Gossard, and D. D. Awschalom, *Appl. Phys. Lett.* **77**, 2379 (2000).
 - ³T. C. Kreutz, G. Zanelatto, E. G. Gwinn, and A. C. Gossard, *Appl. Phys. Lett.* **81**, 4766 (2002); H. Luo, B. D. McCombe, M. H. Na, K. Mooney, F. Lehmann, X. Chen, M. Cheon, S. M. Wang, Y. Sasaki, X. Liu, and J. K. Furdyna, *Physica E (Amsterdam)* **12**, 366 (2002).
 - ⁴H. Ohno, *Science* **281**, 951 (1998); H. Ohno, A. Shen, F. Matsukura, A. Oiwa, A. Endo, S. Katsumoto, and Y. Iye, *Appl. Phys. Lett.* **69**, 363 (1996).
 - ⁵E. J. Singley, R. Kawakami, D. D. Awschalom, and D. N. Basov, *Phys. Rev. Lett.* **89**, 097203 (2002); E. J. Singley, K. S. Burch, J. Stephens, R. Kawakami, D. D. Awschalom, and D. N. Basov, *Phys. Rev. B* **68**, 165204 (2003). K. S. Burch, J. Stephens, R. Kawakami, D. D. Awschalom, D. N. Basov, *Phys. Rev. B* **70**, 205208 (2004).
 - ⁶The method employed here to extract the optical constants of DFHs was first developed at UCSD and is described in Ref. 5. However, this study has provided a number of checks of this method and clearly shows its reliability. First, since DFHs with 10, 25, and 70 ML spacers have the same total thickness, yet different conductivities, we believe all changes in the series are due to changes in the GaAs spacer thickness. The second confirmation can be seen from the excellent agreement between the two samples with 25 ML GaAs spacer thickness. Finally our ability to successfully apply effective medium theory to these samples further confirms its reliability.
 - ⁷The frequency resolution of T_{meas} was kept $\geq 4 \text{ cm}^{-1}$ in order to avoid resolving the interference due to the thick (0.5 mm) substrate. The frequency of these interference fringes were less than 0.5 cm^{-1} . Since we were unable to completely resolve this interference we used a much broader resolution to experimentally smoothen it out. This instrumental smoothing was taken into account in our analysis.
 - ⁸Y. Nagai, T. Kunimoto, K. Nagasaka, H. Nojiri, M. Motokawa, F. Matsukura, T. Dietol, and H. Ohno, *Jpn. J. Appl. Phys., Part 1* **11**, 6231 (2001); M. Linnarsson, E. Janzn, B. Monemar, M. Kleverman, and A. Thilderkvist, *Phys. Rev. B* **55**, 6938 (1997).
 - ⁹The response of the $y=10$ ML sample appears to be gapless based on the data displayed in Fig. 3. Resistivity measurements reported for similar DFH indicate a small increase at low T , see Ref. 3, that can be reconciled with our results assuming that the magnitude of the gap is below the low-frequency cutoff in $\sigma_1(\omega)$ spectra ($\approx 40 \text{ cm}^{-1}$).
 - ¹⁰We note that the EMT is derived assuming the wavelength of the light is much longer than changes in the superlattice and that the interfaces are sharp. For our experiment the wavelength was $\geq 830 \text{ nm}$, while the largest period of the DFH studied was $\approx 20 \text{ nm}$, and variations within the doped layer occur over $\approx 3 \text{ nm}$.
 - ¹¹Y. L. Soo, G. Kioseoglou, S. Kim, X. Chen, H. Luo, Y. H. Kao, Y. Sasaki, X. Liu, and J. K. Furdyna, *Appl. Phys. Lett.* **80**, 2654 (2002).
 - ¹²D. E. Aspnes, *Thin Solid Films* **89**, 249 (1982).
 - ¹³We set $\Omega_c=4500 \text{ cm}^{-1}$ (0.558 eV) based on previous studies of $\text{Ga}_{1-x}\text{Mn}_x\text{As}$. This choice of Ω_c assures the contribution from defect states (As_{Ga}), is small (Ref. 5).
 - ¹⁴Results are similar at all temperatures.
 - ¹⁵ $\sigma_1^{el}(\omega)$ for smaller d_{el} produced qualitatively similar results with overall larger values. TEM studies show the Mn diffuses between 3–5 ML; see Ref. 2.
 - ¹⁶K. Barner *et al.*, *Phys. Status Solidi B* **80**, 451 (1977).
 - ¹⁷J. J. Berry, S. J. Potashnik, S. H. Chun, K. C. Ku, P. Schiffer, and N. Samarth, *Phys. Rev. B* **64**, 052408 (2001).
 - ¹⁸G. L. Carr *et al.*, in *Infrared and Millimeter Waves* edited by Kenneth J. Button (Academic Press, Orlando, 1985), Vol. 13, pp. 171–263.
 - ¹⁹A. van Esch, L. Van Bockstal, J. De Boeck, G. Verbanck, A. S. van Steenberghe, P. J. Wellmann, B. Grietens, R. Bogaerts, F. Herlach, and G. Borghs, *Phys. Rev. B* **56**, 13 103 (1997).
 - ²⁰S. J. Potashnik, K. C. Ku, S. H. Chun, J. J. Berry, N. Samarth, and P. Schiffer, *Appl. Phys. Lett.* **79**, 1495 (2001); K. W. Edmonds, K. Y. Wang, R. P. Champion, A. C. Neumann, N. R. S. Farley, B. L. Gallagher, and C. T. Foxon, *ibid.* **81**, 4991 (2002); T. Hayashi, Yoshiaki Hashimoto, Shingo Katsumoto, and Yasuhiro Iye, *Appl. Phys. Lett.* **78**, 1691 (2001).
 - ²¹M. J. Seong, S. H. Chun, H. M. Cheong, N. Samarth, and A. Mascarenhas, *Phys. Rev. B* **66**, 033202 (2002); K. M. Yu, W. Walukiewicz, T. Wojtowicz, W. L. Lim, X. Liu, Y. Sasaki, M. Dobrowolska, and J. K. Furdyna, *Appl. Phys. Lett.* **81**, 844 (2002); R. Moriya and H. Munekata, *J. Appl. Phys.* **93**, 4603 (2003).
 - ²²N. F. Mott and E. A. Davis, *Electronic Processes in Non-Crystalline Materials* (Clarendon Press, Oxford, 1979).
 - ²³G. Mahieu, P. Condet, B. Grandidier, J. P. Nys, G. Allan, D. Stivenard, Ph. Ebert, H. Shimizu, and M. Tanaka, *Appl. Phys. Lett.* **82**, 712 (2002); T. Tsuruoka, N. Tachikawa, S. Ushioda, F. Matsukura, K. Takamura, and H. Ohno, *ibid.* **81**, 2800 (2002); J. Okabayashi, A. Kimura, O. Rader, T. Mizokawa, A. Fujimori, T. Hayashi, and M. Tanaka, *Phys. Rev. B* **64**, 125304 (2001).
 - ²⁴H. Akai, *Phys. Rev. Lett.* **81**, 3002 (1998); M. Shirai, T. Ogawa, I. Kitagawa, and N. Suzuki, *J. Magn. Magn. Mater.* **177–181**, 1383 (1998); J. H. Park, S. K. Kwon, and B. I. Min, *Physica B* **281**, 703 (2000); J. Inoue, S. Nonoyama, and H. Itoh, *Phys. Rev. Lett.* **85**, 4610 (2000).
 - ²⁵H. A. Fertig and S. Das Sarma, *Phys. Rev. B* **42**, 1448 (1990).
 - ²⁶G. Alvarez and E. Dagotto, *Phys. Rev. B* **68**, 045202 (2003).
 - ²⁷M. Berciu and R. N. Bhatt, *cond-mat/0111045*.
 - ²⁸A. Chattopadhyay, S. Das Sarma, and A. J. Millis, *Phys. Rev. Lett.* **87**, 227202 (2001).
 - ²⁹L. Craco, M. S. Laad, and E. Muller-Hartmann, *Phys. Rev. B* **68**, 233310 (2003).
 - ³⁰J. Fernandez-Rossier and L. J. Sham, *Phys. Rev. B* **64**, 235323 (2001); B. Lee, T. Jungwirth, and A. H. MacDonald, *Semicond. Sci. Technol.* **17**, 393 (2002); S. Sanvito and N. A. Hill, *Phys. Rev. Lett.* **87**, 267202 (2001).